

Production and characterization of dual-phase steels from an AISI 8620 steel with high Mn content

Dayi Gilberto Agredo-Diaz*, Irma Angarita-Moncaleano & Rodolfo Rodríguez-Baracaldo

Universidad Nacional de Colombia, sede Bogotá, Facultad de Ingeniería, Departamento de Ingeniería Mecánica y Mecatrónica, Bogotá, Colombia.
dgradedod@unal.edu.co*, iangaritam@unal.edu.co, rodriguezba@unal.edu.co

Received: September 9th, 2020. Received in revised form: February 1st, 2021. Accepted: February 15th, 2021.

Abstract

Dual phase steels are materials whose microstructure is composed of a ferrite matrix with martensite islands. Ferrite provides excellent ductility, while martensite increases the strength of steel, which provides a special appeal in the automotive industry. The main objective of this research is to obtain dual phase steels from AISI 8620 steel with a high Mn content, using heat treatments in the intercritical range to obtain approximate percentages of martensite of 27, 33, 41, and 48%. Microstructural characterization is performed using optical microscopy and scanning electron microscopy techniques. The mechanical characterization is carried out using hardness, tension and Charpy impact tests. The highest mechanical resistance is achieved in steel with 41% martensite phase, while the highest ductility was obtained by the material with 27% martensite. A fractographic analysis of all materials allowed determining that the type of fracture presented is ductile. When the martensite fraction increases, the impact energy exhibits a decreasing behavior, while the hardness behaves in an increasing way.

Keywords: dual phase steel; martensite; mechanical properties; heat treatment; SEM; fractography.

Producción y caracterización de aceros de fase dual a partir de un acero AISI 8620 con alto contenido de Mn

Resumen

Los aceros de fase dual son materiales cuya microestructura está compuesta de una matriz ferrítica con islas de martensita. La ferrita provee una excelente ductilidad, mientras que la martensita incrementa la resistencia del acero, lo cual es un especial atractivo en la industria automovilística. El principal objetivo de esta investigación es obtener aceros de fase dual a partir de un acero AISI 8620 con alto contenido de Mn, a partir de tratamientos térmicos en el intervalo intercrítico para obtener porcentajes aproximados de martensita de 27, 33, 41 y 48%. La caracterización microestructural es llevada a cabo mediante microscopía óptica y microscopía electrónica de barrido. La caracterización mecánica es realizada por medio de ensayos de dureza, tensión e impacto Charpy. La mayor resistencia mecánica se consiguió en el acero con 27% de martensita. El análisis fractográfico de todos los materiales permitió determinar que el tipo de fractura presentada es dúctil. Cuando la fracción de martensita incrementa, la energía de impacto exhibe un comportamiento decreciente, mientras que la dureza se comporta de forma creciente.

Palabras clave: acero de fase dual; martensita; propiedades mecánicas; tratamiento térmico; SEM; fractografía.

1. Introduction

Dual phase steels are distinguished by their high balance between resistance and ductility. This characteristic is obtained thanks to its microstructure composed of a hard phase (martensite or bainite) dispersed in a ductile ferritic

matrix [1]. The deformation-induced hardening provides a good distribution capacity for these deformations, which favors the ductility of these materials [2]. Likewise, its ability to absorb energy by impact is one of its main attractions in applications for the automotive industry [3]. Another important factor is the high level of fatigue resistance, which,

How to cite: Agredo-Diaz, D.G., Angarita-Moncaleano, I. and Rodríguez-Baracaldo, R., Production and characterization of dual-phase steels from an AISI 8620 steel with high Mn content.. DYNA, 88(217), pp. 42-49, April - June, 2021.

combined with a good energy absorption capacity, makes these steels very attractive for the manufacture of structural parts and as reinforcement in earthquake-resistant applications [4].

Usually, it is necessary to determine thermal or thermomechanical processes that require a biphasic structure (ferrite-martensite, or ferrite-bainite) from commercial steels with a single-phase pearlitic or ferritic structure. This allows opening a range of possibilities by avoiding the use of products that are difficult to access and with high cost [5].

The alloying elements directly affect the type of process that must be applied to obtain a biphasic ferrite-martensite structure. Especially, the incidence of chromium and manganese in obtaining dual phases has not been fully understood. A steel of high industrial consumption and with a high percentage of these elements is AISI 8620, which shows interesting application alternatives in its dual martensite-ferrite phase [6].

In this research, we obtained dual phase steels with martensite contents of 27, 33, 41, and 48% vol from a low alloy AISI 8620 steel with a high Mn content, by applying heat treatments in the inter-critical interval. The aim is to determine the most suitable combination of properties, with a microstructural characterization by optical, scanning electron microscopy and a mechanical characterization using traction, hardness, and impact tests.

2. Materials and methods

A commercial AISI 8620 steel with a high content of Mn is selected. This material is arranged in the form of a 22.2 mm [7/8 in commercial] diameter bar. The determination of the elemental composition of the studied materials was carried out by atomic emission spectroscopy (optical emission spectrometer Baird series DV4).

For the design of the heat treatments (HT), eqs. 1 and 2 were initially taken into account [7] to describe the calculation of the temperatures Ac_1 and Ac_3 . Then, the normalized heat treatment temperature T_n is made to homogenize the microstructure, as shown in eq. 3. After obtaining the temperatures Ac_1 y Ac_3 , the inter-critical temperatures T_i are calculated and the residence times are estimated using the critical treatment radius concept [7,8].

$$Ac_1 = 723 - 10.7(Mn) - 16.9(Ni) + 29.1(Si) + 16.9(Cr) + 290(As) + 6.38(W) \quad (1)$$

$$Ac_3 = 910 - 203\sqrt{C} - 15.2(Ni) + 44.7(Si) + 104(V) + 31.5(Mo) + 13.1(W) \quad (2)$$

$$T_n = Ac_3 + 50^\circ C \quad (3)$$

The heat treatments are carried out in a Lindberg/Blue (Hevi-duty series 5100) electric furnace, thus achieving the necessary temperature ranges with a margin of error of $\pm 5^\circ C$. The processing times selected are in accordance with the critical radius and are the necessary times to achieve the homogenization of the material and its transformation. Fig. 1 shows the general scheme of heat treatment.

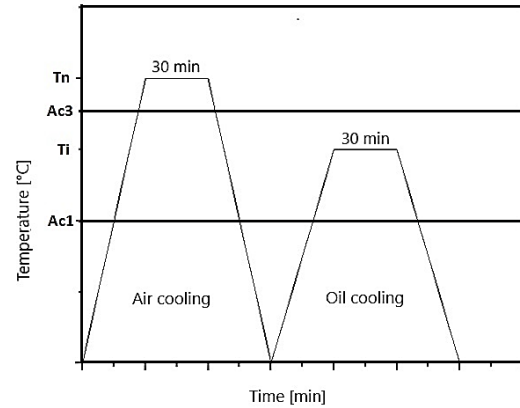


Figure 1. General scheme of the heat treatments carried out. Source: The authors.

The metallographic characterization of the steels was carried out using optical microscopy on a Leco 500 image analyzer, and scanning electron microscopy (SEM) on a Vega3 Tescan electron microscope, the composition by EDS is determined by means of a Bruker XFlash 410-M microsonde coupled to the electron microscope. Conventional polishing is carried out using SiC sandpaper and the microstructure is revealed with 2% nital [9]. Measurements are made for the percentages of phase obtained by optical and electron microscopy, through the digital processing of the images by the ImageJ free software, this is possible given the contrast differences of the metallography [10].

The evaluation of the mechanical and technological properties (property related to the material subject to manufacturing processes) of the material was carried out using hardness, uniaxial tensile and impact tests. For the hardness, the equipment used was an analog Wolpert durometer. The measurements were made on a Rockwell B scale, making a profile of the surface at the center and recording the values every 2 mm, with an error margin of $\pm 5\%$. The tensile tests were carried out with circular specimens of calibrated length of 50 mm according to the ASTM E-8 standard [11]. The equipment used was a Shimadzu UH_X universal testing machine with displacement control at a head speed of 5 mm/min, incorporating an axial traction/compression extensometer. The fracture surface of the specimens submitted to the tensile test is analyzed using scanning electron microscopy. Charpy impact tests are performed under ASTM E-23 standard [12], using a WPM universal impact machine with a sensitivity of 1 kg-m, at an ambient temperature of $21^\circ C$ and relative humidity of 49% (environmental conditions are measured with a thermohygrometer HTC2).

3. Results and discussion

3.1. Heat treatments

The elemental composition of the study material shows a steel with 1.099% Mn, which is in accordance with ASTM A29 standard [13]. The manganese content range (Mn) is between 0.7 and 0.9% in weight. Roy et al. [14] refer to this same steel composition as AISI 8620 with high manganese and low content of alloying elements. Table 1 summarizes the percentages of the main elements that comprise the study material.

Table 1.
Elemental composition of the study material. Weight percentage.

C	Si	Cr	Mn	Mo	Ni	Fe
0.214	0.272	0.935	1.099	0.013	0.029	Balance

Source: The authors.

Table 2.
Treatment temperatures.

Heat treatment (% of phase proposed)	Temperature (°C)	Time (min)
Normalized	900	
Heat treatment 1 (HT1 20% martensite)	765	
Heat treatment 2 (HT2 30% martensite)	780	30
Heat treatment 3 (HT3 40% martensite)	790	
Heat treatment 4 (HT4 50% martensite)	805	

Source: The authors.

Following the methodology, the treatment temperatures are obtained. Table 2 summarizes the calculations of the temperatures of normalized and intercritical heat treatment for the different percentages of the phase proposed.

3.2. Metallographic characterization

Optical microscopy results for the as-received material show a microstructure of ferrite and pearlite grains [15]. This condition is evidenced in Fig. 2a. Since the study material comes from a rod, it has a deformed grain structure that needs to be homogenized. Fig. 2b shows the homogenized material with a decreased grain size, as a result of the normalized heat treatment.

Fig. 3 shows the microstructure of the steel by optical microscopy after the heat treatments.

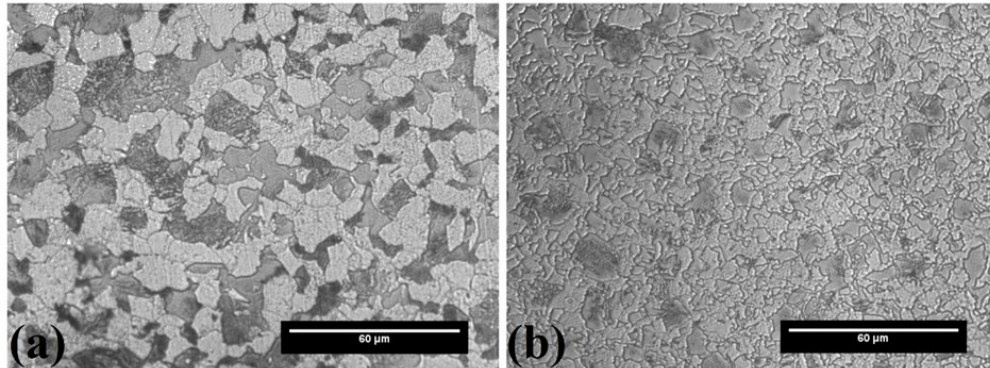


Figure 2. Steel microstructure: (a) in as-received state (AS) and (b) with normalized heat treatment. 2% nital.
Source: The authors.

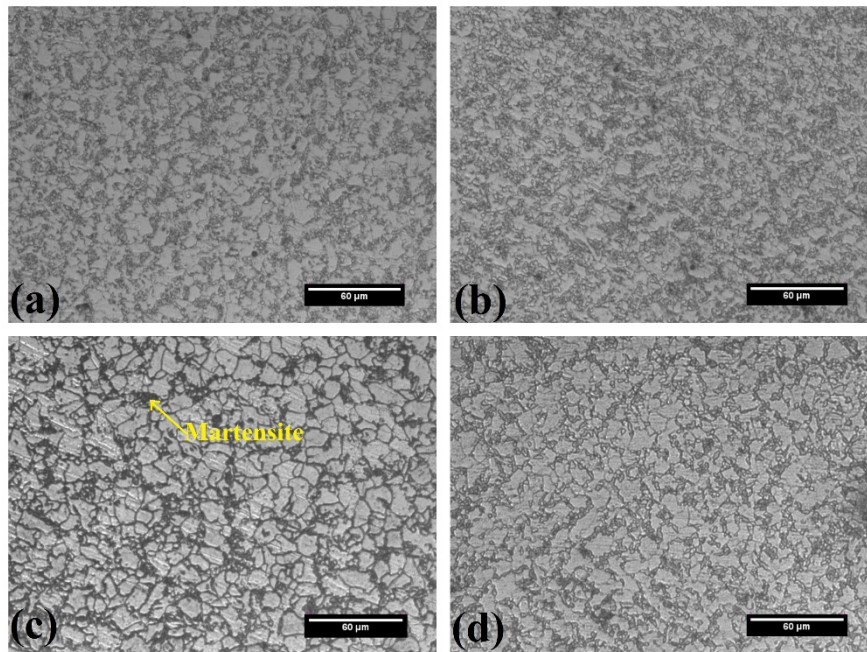


Figure 3. Microstructures obtained by optical microscopy of the material with heat treatment: (a) HT1, (b) HT2, (c) HT3 and (d) HT4. 2% nital.
Source: The authors.

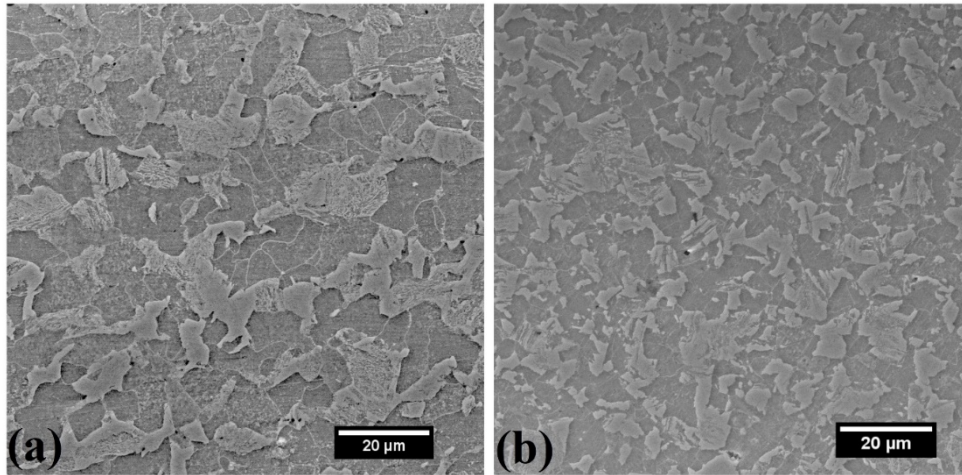


Figure 4. Microstructure of the material in SEM with secondary electrons (SE): (a) in raw state and (b) with normalized heat treatment. 2% nital.
Source: The authors.

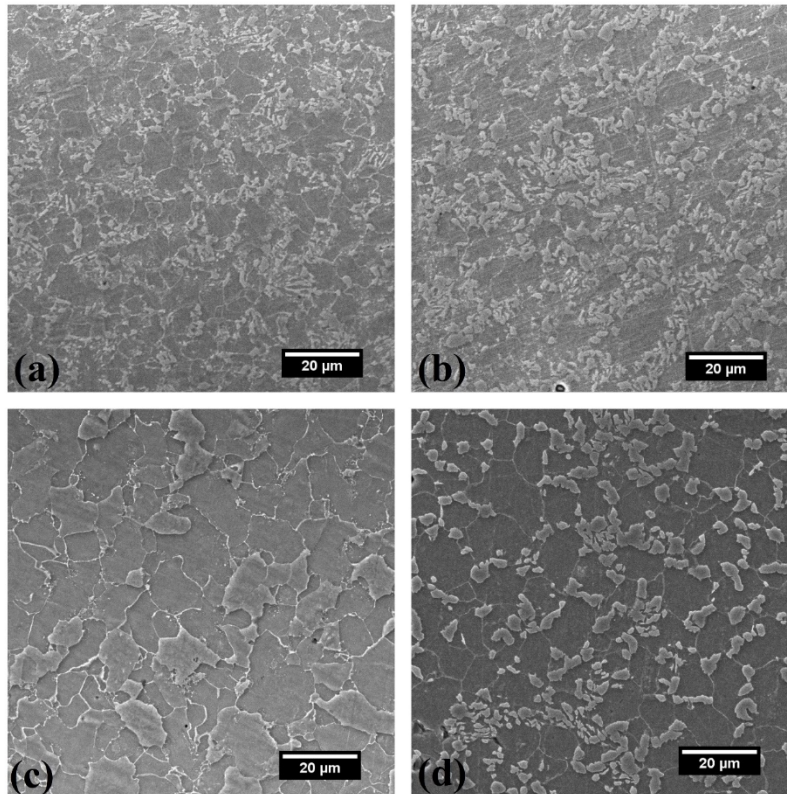


Figure 5. Microstructures obtained by SEM results of heat treatments: (a) HT1, (b) HT2, (c) HT3 and (d) HT4. 2% nital.
Source: The authors.

According to the established methodology, it is possible to obtain different martensite fractions through treatment in the intercritical zone. This fraction increases as the energy in the treatment increases, which is observable in the images of the treated steels where the grain size is stable^[14].

Fig. 4 shows the microstructures obtained by the scanning electron microscopy technique. Fig. 4a

corresponds to the microstructure of the material in as-received state (AS). Fig. 4b shows the microstructure of the material after the normalized heat treatment, thus showing a condition of homogeneity of the ferrite and pearlite phases.

Fig. 5 shows the microstructures by SEM, with results of the heat treatments HT1, HT2, HT3, and HT4. In general terms, the images show a dual microstructure of ferrite with martensite islands.

Table 3.
Martensite fraction: theoretical and obtained by treatment.

Theoretical martensite fraction (%)	Real martensite fraction (%)	Standard deviation	Absolute error	Relative error (%)
20	27.34	1.35	7.34	36.68
30	32.98	1.44	2.98	9.92
40	41.53	1.13	1.12	1.13
50	48.42	1.45	1.59	3.17

Source: The authors.

In the intercritical zone, it is possible to predict the percentages of phase combination with the adequate use of the lever rule. The normalized heat treatment is necessary to homogenize the grain structure and refine it. After the thermal treatment, the increase in temperature did not generate grain growth. Grain stability is influenced by the high percentage of Mn (1.099% wt), as observed by Calcagnotto et al. [18]. The metallography results for the material in as-received state show a microstructure of ferrite and pearlite with an average hardness of 83 HRB. The microstructure of the heat-treated materials shows their transformation into a ferrite distribution with martensite islands, where the more energy is supplied in the heat treatment, the higher fraction of martensite is obtained. Similar results were obtained in the work by Lorusso et al. [13]. The metallography results show no presence of other phases, which is a consequence of the Mn content that facilitates the transformation of austenite into martensite [18].

The percentage of the martensite phase is measured for the heat treatments carried out. Table 3 summarizes these results, which are the product of the statistical treatment with 60 measurements for each treatment. The greatest variation of the martensite fraction is given for 20% theoretically, since there is a greater amount of carbon available in the martensite phase when it is in a lower volumetric proportion, which makes the transformation more difficult to control.

3.3. Mechanical characterization

Fig. 6 shows the results of hardness for the thermally treated materials. They present a constant characteristic from the surface to the center, which corroborates the good homogeneity achieved with the treatments.

There is a direct relationship of hardness with the percentage of phase. As the energy in the treatment is increased, the percentage of martensite rises and the hardness of the material increases. This observation was also presented in various works on dual phase steels [16,17,19-22].

Results of the tensile test are shown in Fig. 7. Table 4 summarizes the mechanical properties extracted from the stress-strain curves for the different percentages of martensite obtained.

The maximum and yield strength of the material increases in the HT3 treated sample concerning the steel in as-received state, due to the presence of the martensite phase. At the maximum stress values, the greatest differences between steels occur. This reflects different levels of hardening capacity in the plastic region of the material and is linked with an increase in the density of dislocations formed during the transformation process of austenite in martensite. Kumar et al. [23] established in their work the dependence of the amount of martensite on the increasing the resistance of the material, that is, the degree of deformation depends on the volume fraction and the carbon content in the martensite phase.

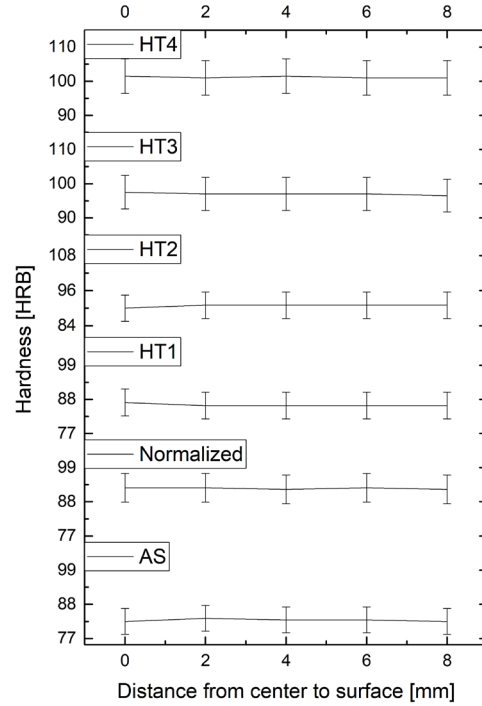


Figure 6. Hardness from center to surface for AS and heat-treated materials. Source: The authors.

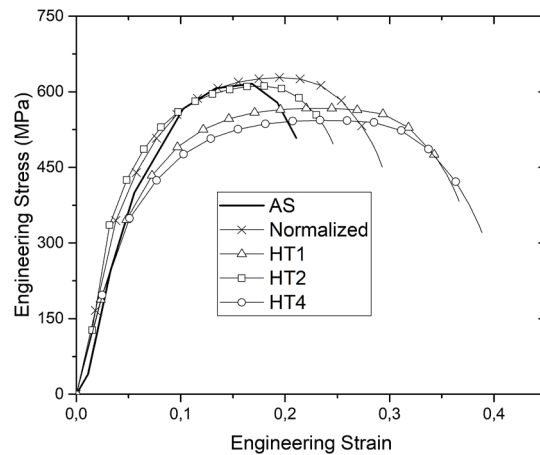


Figure 7. Stress-strain curve for heat-treated materials. Source: The authors.

Table 4.
Tensile test results.

	Martensite fraction [%]	Maximum stress [MPa]	Yield stress [MPa]	Uniform elongation [%]	Total elongation [%]
AS		617.74	306.10	4.07	15.78
Normalized		628.64	336.72	3.57	19.84
HT1	27	567.70	279.55	3.25	23.51
HT2	33	611.89	297.42	2.66	17.84
HT3	41	754.72	419.14	4.10	10.50
HT4	48	544.33	301.96	3.61	23.21

Source: The authors.

The difference between yield and maximum stress shows the significant deformation hardening capacity of these materials. Another relevant factor to consider is the carbon content of the material. Although carbon is fixed, there is greater availability when you have a lower fraction of martensite. In this work, the trend of the mechanical resistance values due to treatments carried out on steel have a direct correspondence with the investigations carried out by Pandre et al. [24]. However, these authors work with a lower carbon content material, thus presenting lower mechanical resistance values.

The material with heat treatment to produce 27% martensite shows the best behavior between resistance and ductility with a uniform elongation of 3.248% and an increase in the total elongation of 7.724% compared with the material in as-received state. For 41% of martensite, the resistance increases by 18.16%, with a decrease in the total elongation of 33.47%, compared with the material in as-received state.

Fig. 8 shows the micro-mechanism of fracture produced by the tensile test for untreated and treated materials. Examination of the surface reveals a ductile dimpled fracture for the AS and the 4 treatments. The phenomenon of microcavity formation can be observed, where the dominant nature of the fracture is ductile. This predominant ductile mechanism was also pointed out by Ahmad et al. [25], and modeled in the work of Rana et al. [23].

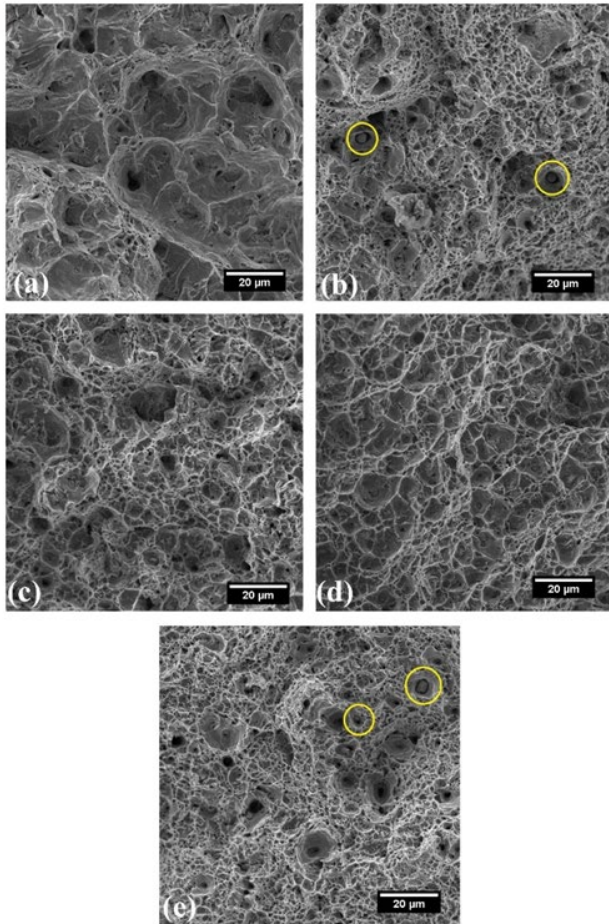


Figure 8. SEM fractography images for as-received and heat-treated materials: (a) AS, (b) HT1, (c) HT2, (d) HT3, (e) HT4. Yellow circles: Fe-Mn compounds.
Source: The authors.

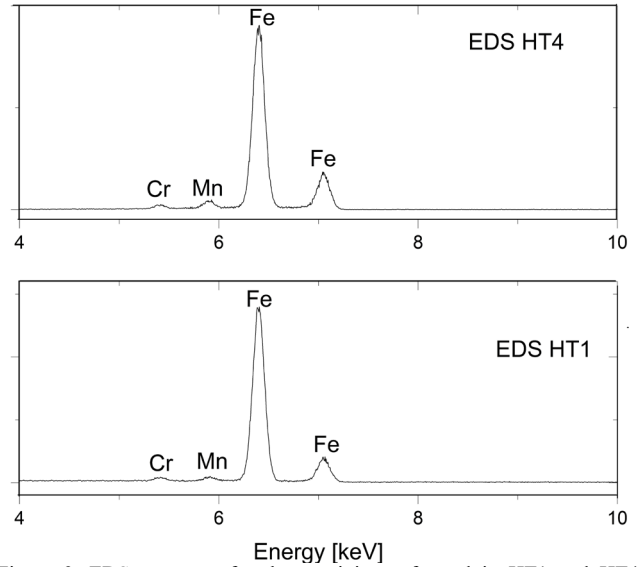


Figure 9. EDS spectrum for the precipitates formed in HT1 and HT4, respectively.

The specimens with HT1 and HT4 treatment evidence particles that originate larger microcavities (highlighted with yellow circles, Figs. 8b and 8e). An analysis is performed using X-ray energy dispersion spectrometry (EDS). These results are illustrated in Fig. 9, and evidence the presence of Fe-Mn compounds, mainly for the two treatments.

The fractographic study reveals the fracture micromechanism of each of the samples, where a ductile fracture with microvoid formation dominates (Fig. 8), obtaining a higher maximum stress and yield stress condition for the HT3. The thermal treatments HT1, HT2, and HT4, exhibit the presence of larger microcavities, this is linked to a condition of greater ductility, these results agree with that reported in [25-27], while the HT3 evidences a less ductile fracture characteristic linked to greater maximum stress, so that the resulting surfaces present undulations characteristic of a plastic decohesion mechanism, a condition clearly detectable in electronic fractography [28]. On the other hand, the materials whose treatments are HT1 and HT4, evidence the formation of precipitates, which favors the formation of larger microcavities, with smaller cavities around them, this is because there are fewer nucleation sites in microcavities, this condition is studied in the references [5,29,30].

The results of the impact test shown in Fig. 10 generally show a decrease in impact toughness with increasing martensite fraction. For HT1 it has the highest energy absorption, reporting an average value of 231.45 J, this increase in toughness is linked to the presence of mostly ferrite, which is the soft phase and high toughness, this same trend of reported fuel by Kadkhodapour et al. [17]. A decrease in impact energy is evident for the material whose microstructure is made up of 49% martensite, obtaining a value of 16.08 J, this is linked to the fact that when there is a higher fraction of martensite, the cracks tend to spread more in the ferrite-martensite interface, causing toughness to decrease.

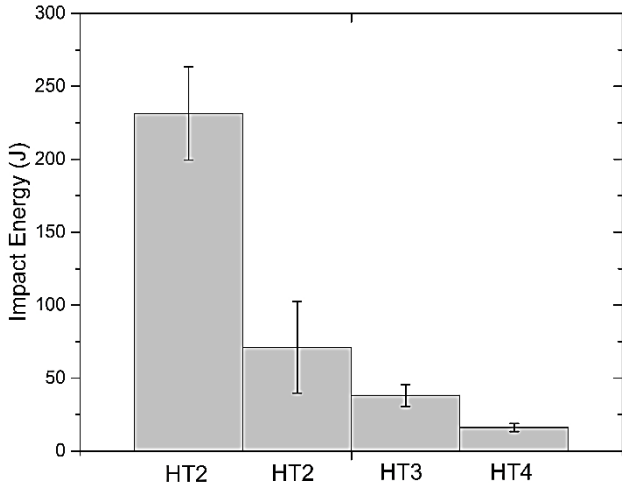


Figure 10. Impact energy for heat treated materials. Source: The authors.

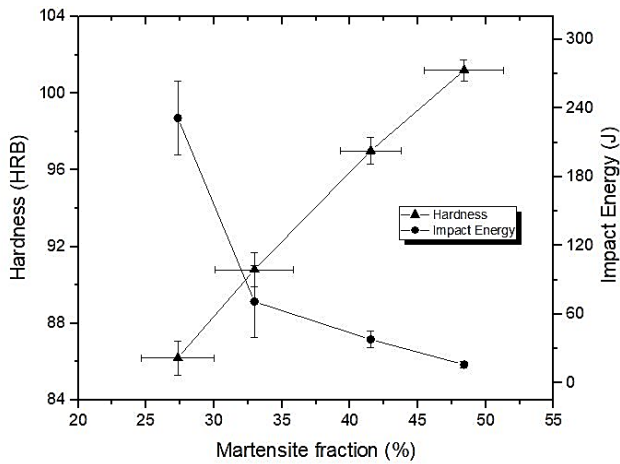


Figure 11. Hardness and impact energy depending on the martensite fraction. Source: The authors.

Fig. 11 shows the relationship between impact energy, hardness, and the martensite fraction. The impact energy exhibits a decreasing behavior, while the hardness increases with the martensite fraction. This shows an inversely proportional relationship between the two properties and agrees with studies carried out by Sun et al. [20], which emphasizes the morphology of martensite, and Calcagnotto et al., who researched in depth the size of this phase [22].

4. Conclusions

From an AISI 8620 steel, it was possible to design heat treatments to obtain ferrite-martensite dual-phase steel with specific percentages of each phase and low relative errors. The presence of high Mn content (1.099% wt) showed an adequate control of grain growth during the heat treatments and facilitated its transformation to martensite.

The highest mechanical resistance condition occurs for steel produced by heat treatment 3, with 41% martensite; while the highest ductility is obtained for steel produced in

heat treatment 1, with a fraction of 27 % martensite.

The fractographic analysis carried out at different levels of magnification made it possible to determine the fracture mechanism in the materials studied. They presented in general a ductile fracture with the formation of microcavities, whose geometry varies depending on the type of treatment.

Steels produced by heat treatment have a good condition of homogeneity in their microstructure. The hardness of the materials is constantly present from the core to the surface with a linear trend depending on the martensite fraction.

The presence of Fe-Mn compounds favors the formation of larger microcavities, with a higher density of smaller cavities around them. This condition is linked with the fact that there are fewer nucleation sites.

Increasing the fraction of the martensite phase evidences a decreasing behavior in the impact energy, while hardness exhibits an increasing behavior.

Acknowledgements

Special thanks to the Department of Mechanics and Mechatronics Engineering of the School of Engineering at Universidad Nacional de Colombia, campus Bogotá, for the advice of their teachers, provision of laboratories, and promoting research at undergraduate and postgraduate levels.

References

- [1] Caprili, S., Salvatore, W., Valentini, R., Ascanio, C. and Luvarà, G., A new generation of high-ductile Dual-Phase steel reinforcing bars. *Constr. Build. Mater.*, 179, pp. 66-79, 2018. DOI: 10.1016/j.conbuildmat.2018.05.181.
- [2] Monsalve, A., Artigas, A., Castro, F., Colás, R. and Houbaert, Y., Characterization of dual-phase steels obtained by hot-rolling. *Rev. Metal.*, pp. 1-10, 2010. DOI: 10.3989/revmetalmadrid.0914.
- [3] Rodríguez-Baracaldo, R., Arroyo-Osorio, J.M. y Parra-Rodríguez, Y., Influencia del proceso de revenido en el comportamiento mecánico de un acero de fase dual de uso industrial automotriz. *Ingeniare*, 24(1), pp. 94-101, 2016. DOI: 10.4067/S0718-33052016000100009.
- [4] Apostolopoulos, C.A., Mechanical behavior of corroded reinforcing steel bars S500s tempcore under low cycle fatigue. *Constr. Build. Mater.*, 21(7), pp. 1447-1456, 2007. DOI: 10.1016/j.conbuildmat.2006.07.008.
- [5] Saeidi, N. and Ekrami, A., Comparison of mechanical properties of martensite/ferrite and bainite/ferrite dual phase 4340 steels. *Mater. Sci. Eng. A*, 523(1-2), pp. 125-129, 2009. DOI: 10.1016/j.msea.2009.06.057.
- [6] Erdogan, M. and Tekeli, S., The effect of martensite volume fraction and particle size on the tensile properties of a surface-carburized AISI 8620 steel with a dual-phase core microstructure. *Mater. Charact.*, 49(5), pp. 445-454, 2002. DOI: 10.1016/S1044-5803(03)00070-6.
- [7] Krauss, G., *Processing, Structure, and Performance*. 2005.
- [8] Castillo-Gutiérrez, D.E., Angarita-Moncaleano, I.I. and Rodríguez-Baracaldo, R., Caracterización microestructural y mecánica de aceros de fase dual (ferrita-martensita), obtenidos mediante procesos térmicos y termomecánicos. *Ingeniare. Rev. Chil. Ing.*, 26(3), pp. 430-439, 2018. DOI: 10.4067/s0718-33052018000300430.
- [9] Agredo-Diaz, D.G. et al., Effect of a Ni-P coating on the corrosion resistance of an additive manufacturing carbon steel immersed in a 0.1 M NaCl solution. *Mater. Lett.*, 275, art. 128159, 2020. DOI: 10.1016/j.matlet.2020.128159.
- [10] Schneider, C.A., Rasband, W.S. and Eliceiri, K.W., NIH Image to ImageJ: 25 years of image analysis. *Nat. Methods*, 9(7), pp. 671-675, 2012. DOI: 10.1038/nmeth.2089.

- [11] ASTM Int. Standard Test Methods for Tension Testing of Metallic Materials 1 - ASTM E8M-13a. Astm, (C), pp. 1-28, 2014. DOI: 10.1520/E0008.
- [12] ASTM Int. ASTM E23 – 18, Standard Test Methods for Notched Bar Impact Testing of Metallic Materials. ASTM Int., pp. 1-26, 2018. DOI: 10.1520/E0023-18.
- [13] ASTM Int. Standard Specification for General Requirements for Steel Bars, Carbon and Alloy, Hot-Wrought. Changes, I(September), 1999, pp. 1-16, 2009. DOI: 10.1520/A0029.
- [14] Roy, S., Zhao, J., Shrotriya, P. and Sundararajan, S., Effect of laser treatment parameters on surface modification and tribological behavior of AISI 8620 steel. *Tribol. Int.*, 112(December), 2016, pp. 94-102, 2017. DOI: 10.1016/j.triboint.2017.03.036.
- [15] Vander Voort, and Baldwin, W., *Metallography and Microstructures Handbook*. ASM Int., 9, art. 2733, 2004. DOI: 10.1361/asmhba0003771.
- [16] Lorusso, H., Burgueño, A. y Svoboda, H.G., Propiedades mecánicas y caracterización microestructural de diferentes acero dual-phase. in: 2008 - Conamet - Sam, CONAMET/SA, no. 1, 2008, 8 P.
- [17] Kadkhodapour, J., Schmauder, S., Raabe, D., Ziacci-Rad, S., Weber, U. and Calcagnotto, M., Experimental and numerical study on geometrically necessary dislocations and non-homogeneous mechanical properties of the ferrite phase in dual phase steels. *Acta Mater.*, 59(11), pp. 4387-4394, 2011. DOI: 10.1016/j.actamat.2011.03.062.
- [18] Calcagnotto, M., Ponge, D. and Raabe, D., On the effect of manganese on grain size stability and hardenability in ultrafine-grained ferrite/martensite dual-phase steels. *Metall. Mater. Trans. A Phys. Metall. Mater. Sci.*, 43(1), pp. 37-46, 2012. DOI: 10.1007/s11661-011-0828-3.
- [19] Zhang, J., Di, H., Deng, Y. and Misra, R.D., Effect of martensite morphology and volume fraction on strain hardening and fracture behavior of martensite-ferrite dual phase steel. *Mater. Sci. Eng. A*, 627, pp. 230-240, 2015. DOI: 10.1016/j.msea.2015.01.006.
- [20] Sun, S. and Pugh, M., Properties of thermomechanically processed dual-phased steels containing fibrous martensite. *Mater. Sci. Eng. A*, 335(1-2), pp. 298-308, 2002. DOI: 10.1016/S0921-5093(01)01942-6.
- [21] Calcagnotto, M., Adachi, Y., Ponge, D. and Raabe, D., Deformation and fracture mechanisms in fine- and ultrafine-grained ferrite/martensite dual-phase steels and the effect of aging. *Acta Mater.*, 59(2), pp. 658-670, 2011. DOI: 10.1016/j.actamat.2010.10.002.
- [22] Calcagnotto, M., Ponge, D. and Raabe, D., Effect of grain refinement to 1µm on strength and toughness of dual-phase steels. *Mater. Sci. Eng. A*, 527(29-30), pp. 7832-7840, 2010. DOI: 10.1016/j.msea.2010.08.062.
- [23] Rana, A.K., Paul, S.K., and Dey, P.P., Effect of martensite volume fraction on cyclic plastic deformation behavior of dual phase steel: micromechanics simulation study. *J. Mater. Res. Technol.*, 8(5), pp. 3705-3712, 2019, DOI: 10.1016/j.jmrt.2019.06.022.
- [24] Pandre, S., Takalkar, P., Kotkunde, N., Singh, S.K. and Haq, A.U., Influence of temperatures and strain rates on tensile deformation behaviour of DP 590 steel. *Mater. Today Proc.*, 18, pp. 2603-2610, 2019, DOI: 10.1016/j.matpr.2019.07.119.
- [25] Ahmad, E., Manzoor, T., Hussain, N. and Qazi, N.K., Effect of thermomechanical processing on hardenability and tensile fracture of dual-phase steel. *Mater. Des.*, 29(2), pp. 450-457, 2008, DOI: 10.1016/j.matdes.2006.12.022.
- [26] Avendaño-Rodríguez, D., Granados, J.D., Espejo-Mora, E., Mujica-Roncery, L. and Rodríguez-Baracaldo, R., Fracture mechanisms in dual-phase steel: Influence of martensite volume fraction and ferrite grain size. *J. Eng. Sci. Technol. Rev.*, 11(6), pp. 174-181, 2018, DOI: 10.25103/jestr.116.22.
- [27] Liu, W., Lian, J. and Münstermann, S., Damage mechanism analysis of a high-strength dual-phase steel sheet with optimized fracture samples for various stress states and loading rates. *Eng. Fail. Anal.*, 106(July), art. 104138, 2019, DOI: 10.1016/j.engfailanal.2019.08.004.
- [28] Ipohorsky, M. and Acuña, R., *Fractografía. Aplicaciones al análisis de fallas*. Com. Nac. Energ. At., 69, pp. 363-377, 1988.
- [29] Ipohorski, M., *Fractografía electrónica: su contribución al análisis de falla*. Rev. SAM, 1(2), pp. 1-42, 2004.
- [30] Cenoz-Echeverría, I. and Fernández-Carrasquilla, J., Influence of the composition and heat treatments in the mechanical properties of aluminium bronze alloys. *Rev. Metal.*, 43(4), pp. 272-283, 2007, DOI: 10.3989/revmetalm.2007.v43.i4.73.

D.G. Agredo-Diaz, is a BSc. Eng. in Mechanical Engineer from Universidad Nacional de Colombia (2019). He is currently pursuing a MSc. degree in Materials and Processes at Universidad Nacional de Colombia and is registered as a researcher and assistant professor. He joined as an intern at Universidad Nacional Autónoma de México (2018) in the Centro de Ingeniería de Superficies y Acabados (CENISA). Prof. Agredo is a member of the Surface Engineering and Tribology Network (REDISYT). His research interests are materials processing, corrosion and wear, electrochemical techniques, surface engineering, and educational topics. ORCID: 0000-0003-2830-3022

I. Angarita-Moncaleano, received the BSc. Eng. as Mechanical Engineer from the Universidad Nacional de Colombia in 1993, MSc. in Materials and Processes from the same university and a PhD. in Engineering and Industrial Production from the Polytechnic University of Valencia, Spain. She is a professor in the area of Materials and Processes and she works at Universidad Nacional de Colombia since 2001. She conducts research in the area of powder metallurgy, heat treatments and characterization of materials. ORCID: 0000-0002-2674-6893

R. Rodríguez-Baracaldo, received the BSc. Eng. in Mechanical Engineering in 1997, from the Universidad Nacional de Colombia, the MSc. in Mechanical Engineering in 1999, and the PhD. in Materials Engineering and Metallurgy in 2008 from the Universidad Politécnica de Cataluña, (España). He has worked for Universidad Nacional de Colombia since 2000. Currently, he is a full professor in the Department of Mechanics and Mechatronics Engineering, School of Engineering, Universidad Nacional de Colombia. His research interests include mechanical metallurgy, mechanical properties of advanced materials, metal forming, and computational materials: modeling and simulation. ORCID: 0000-0003-3097-9312